Journal of Sound and Vibration 329 (2010) 4136–4148

Contents lists available at ScienceDirect

Journal of Sound and Vibration

journal homepage: www.elsevier.com/locate/jsvi

A study on the characteristic behavior of mass inclusions added to a poro-elastic layer

Kamal Idrisi [a,*], Marty E. Johnson [c], Daniel Theurich [d], James P. Carneal [b]

[a] Mercedes Technology Center, HPC 059/X631, 71059 Sindelfingen, Germany
[b] GE Energy, 3901 Castle Hayne Road, Wilmington, NC 28401, USA
[c] 143 Durham Hall, 24060 Blacksburg VA, USA
[d] MTU Aero Engines, Dachauer Str. 665, 80995 Munich, Germany

ARTICLE INFO

Article history:
Received 11 October 2008
Received in revised form
30 March 2010
Accepted 5 April 2010
Handling Editor: M.P. Cartmell
Available online 26 May 2010

ABSTRACT

Heterogeneous (HG) blankets consist of a layer of poro-elastic media with small embedded masses that replicate the behavior of a distributed mass–spring–damper system. The concept of an HG blanket used to control the sound transmission through an aircraft double-panel system has already been developed and cited in the present literature. However, deficiencies in methodical property control exist; therefore, the prime objective of this research is to provide a simple method to predict and control material properties of the heterogeneous blankets through alteration of mass and stiffness parameters. Mass inclusion size, shape, and placement were varied. If optimized heterogeneous (HG) blankets targeted to specific applications are to be successfully developed, control of these parameters is necessary.

This research offers a detailed analysis of the behavior of the mass inclusions, highlighting controlled stiffness variation of the mass–spring–damper systems inside the HG blanket. Characteristic parameters of the HG blanket like the "footprint," "effective area," and the "mass interaction distance" are defined and confirmed through mathematical calculations and experimental results. A novel, empirical approach to predict the natural frequency of different mass shapes embedded in porous media was derived and experimentally verified for many different types of porous media, including melamine foam, polyurethane, and polyamide. A maximum error of 8% existed for all the predictions made in this document.

1. Introduction

This study provides an in-depth examination of the behavior of heterogeneous (HG) blankets designed to reduce the vibration and sound transmission through double-panel aircraft structures (as shown in Fig. 1). HG blankets use small mass inclusions placed inside a poro-elastic blanket, creating small mass–spring–dampers that can control sound transmission at low frequencies. This document concentrates on predicting and controlling the behavior of these mass inclusions. Although the concept of an HG blanket has been fully defined in the present literature, deficiencies in methodical property control exist. The prime objective of this research is to provide a simple method to predict and control

* Corresponding author. Tel.: +49 0 7031/90 44506.
E-mail addresses: kamal.idrisi@daimler.com (K. Idrisi), martyj@vt.edu (M.E. Johnson), daniel.theurich@mtu.de (D. Theurich), jcarneal@yahoo.com (J.P. Carneal).

0022-460X/$ - see front matter © 2010 Elsevier Ltd. All rights reserved.
doi:10.1016/j.jsv.2010.04.001

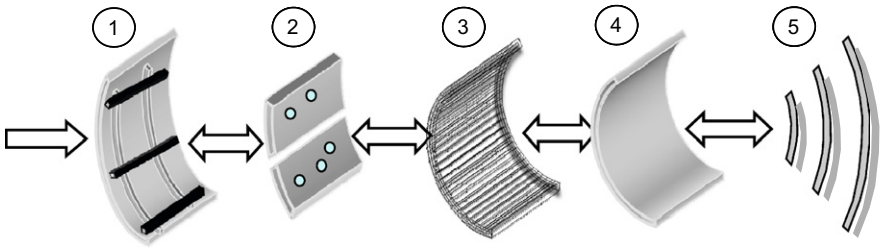

Fig. 1. Schematic of the double-panel system to be optimized: (1) fuselage, (2) HG blanket, (3) air cavity, (4) trim, and (5) interior acoustic field.

the characteristics of the small mass–spring–dampers through alteration of the material properties of the porous media and alterations in the size, the shape, and the placement of the mass inclusions.

The control of low-frequency noise in aircraft [1] is a challenge due to the weight and the thickness restrictions imposed on any acoustic treatment. Typically the thickness of a passive noise control treatment limits the bandwidth over which the treatment will be effective. For example, Baumgartl [2] presented the sound absorbance as a function of wave frequency for several thicknesses of melamine foam as a function of frequency and showed that the absorbance was highly dependent upon the thickness of the treatment. Thick layers were also required for the absorption of low frequencies. For instance, the degree of sound absorption for 50 mm thick foam at 500 Hz is 0.5 and drops down rapidly to an absorption value of 0.05 at 100 Hz. Therefore, passive treatments positioned inside the fuselage shell of an aircraft, where the fuselage dimensions limit the thickness of the blankets to a few inches, causes the acoustic blankets to be ineffective at frequencies below about 500 Hz [3,4]. In view of this finding, many researchers have suggested active techniques as a solution [5–7], but these systems are often too complex and unreliable for practical use. As an alternative, HG blankets have been suggested as a passive solution to this problem and have shown great potential.

In the present literature, the HG blanket concept evolved through a series of steps, starting with a single-point absorber (as shown in Fig. 2(I)), extending to multiple absorbers acting over a distributed space (Fig. 2(II) and Ref. [8]), extending further to multiple masses coupled together (Fig. 2(III) and Refs. [9,10]), and finally broadening to the full HG concept. In the full HG concept, multiple mass inclusions are placed inside a continuous (porous) media to simulate a distributed mass–spring–damper system (Fig. 2(IV)) that operates at low frequency where the blanket is no longer an effective passive absorber. By employing an acoustic treatment (i.e. the porous media) to provide the stiffness for the mass inclusions, the HG blanket concept combines both the main types of passive control mechanisms, damping (high frequencies) and dynamic absorption (low frequencies), into a single treatment designed to control a wide frequency range. The acoustic treatment, or porous media, is a complex structure with coupled fluid and solid properties [11]. However, in the low-frequency regime where the mass inclusions resonate, the polymer matrix or foam provides the majority of the stiffness that acts against the mass inclusions. With appropriate design, the resonances of the small embedded masses can be used to control the low-frequency vibration of a structure as depicted in Fig. 3(a).

Kidner et al. [12] as well as Sgart Atalla, and Amedin [13,14] recently demonstrated that HG blankets have significant potential to reduce low-frequency-radiated sound from structures. Kidner et al. generalized that HG blanket efficiency increases when the masses are positioned to target certain modes rather than using a random distribution. In order to target a plate mode, the embedded mass is tuned to the desired frequency and positioned at the anti-node of the targeted mode. Proper tuning of the masses will result in a mode split from the targeted resonance of the base structure.

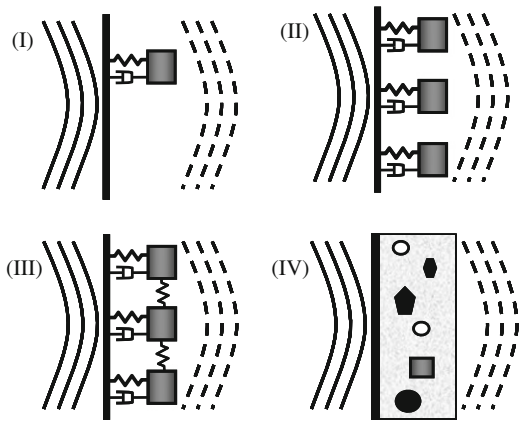

Fig. 2. Schematic of the development of the HG blanket. Schematic of the development of the HG blanket: single-point absorber (I), multiple absorbers acting over a distributed space (II), multiple masses coupled together (III), and HG blanket (IV).

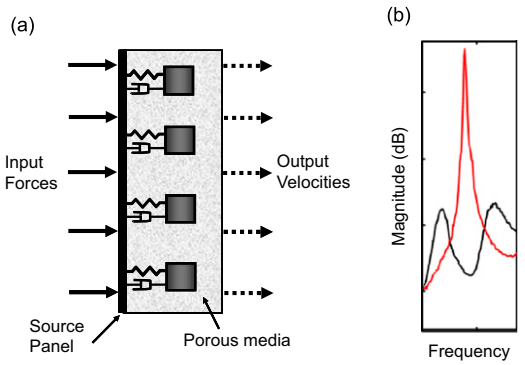

Fig. 3. Schematic of the plate with HG blanket mounted on top (a) and schematic of the damped mode split effect of the HG blanket, before (– – – –) and after (——) targeting base structure mode (b).

In accordance with traditional tuned vibration absorber theory [15], the targeted resonance peak splits into two peaks, one above and one below the original peak. If the damping ratio is correctly designed [16,17], both resultant resonant frequencies have lower and more damped amplitudes than the original resonance (Fig. 3(b)).

Previous literature confirms that the resonance frequency of the mass inclusion varies with depth [12]. However, this manuscript shows that other parameters including the shape of the inclusion also affect the resonance frequency and can be used to tune the device. An objective of this research is to outline novel techniques for predicting and tuning the resonance frequencies of the mass inclusions. A parametric analysis of mass inclusion behavior is presented, probing both mass and stiffness variations inside the HG blanket with a mass–spring–damper model. Experimental and calculated innate parameters of the HG blanket like the "footprint," "mass interaction distance," and "effective area" are then defined. In this paper, an empirical approach is found and used to predict the natural frequencies of different mass shapes embedded in porous media and is shown to be accurate within 8% over a range of porous materials and mass shapes.

2. FE model and experimental investigation

This section presents the finite element (FE) model and experimental setup used to analyze the HG blanket characteristics and the behavior of the mass inclusions. FE results are used in cases where experimental results are difficult to obtain. The FE model of the HG blanket is based on fundamental fluid, structural, and coupled fluid–structural equations (schematic shown in Fig. 2).

2.1. FE model

The details of the finite element code used for this work are well-presented elsewhere in the literature; therefore, this section will only provide a brief description of the relevant literature and explain how the model was used for this work.

Panneton and Atalla [18] proposed a poro-elastic FE derivation based on fundamental poro-elastic material properties derived by Biot [19], and this was further developed by Allard [20]. Gautam [21] expanded the scheme to include mass inclusions (i.e. modeled HG blankets). The authors adapted this code to analyze sound transmission through a double-panel system with a sandwiched HG blanket and have validated it experimentally [22,23]. For this work the FE model of the HG blanket was used to analyze the interaction between the mass and a block of foam (melamine #1a in Table 1). Mass inclusions were placed at single nodes in the FE mesh [13,14], and the stress and displacement fields generated by the masses could then be calculated. The foam block was excited with a uniform velocity over its base. Thus, each node at the base was driven with a constant unit velocity. Transfer functions between the input base velocity and the nodes corresponding to mass inclusions could then be used to investigate the characteristics of the masses (such as natural frequency and damping). In addition, the stress fields created by the excited masses could also be investigated.

Table 1
Model parameters of the FE model of an HG blanket.

Poro type	Modulus of elasticity (N/m^2)	Density (kg/m^3)	Flow resistivity ($N\,s/m^4$)
Melamine #1a (white)	4.76×10^5	8.44	1.14×10^4
Melamine #2 (grey)	3.83×10^5	9.07	0.99×10^4
Polyurethane	1.05×10^5	28.98	1.3×10^4
Polyamide	3.0×10^5	7.86	35.3×10^4

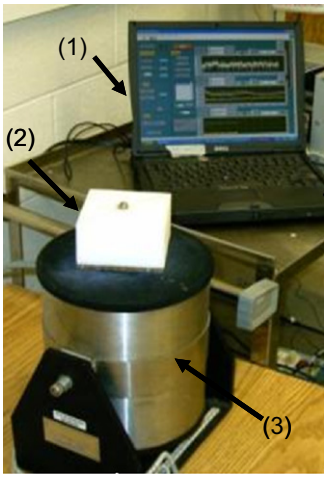

Fig. 4. Experimental setup to measure the natural frequencies of the mass inclusions inside the HG blanket. Shown is the data acquisition system (1), the HG blanket, (2) and the shaker (3).

2.2. Experimental investigation

To study the fundamental behavior of one mass inclusion, block of porous material with a single mass inclusion was used to determine the natural frequencies and damping of the HG blanket. The test could then be repeated for various masses (various shapes and weights). The mass inclusion was either glued on top of the porous block or inserted into the middle of the block after cutting the block in two pieces (half of the depth). The two pieces were subsequently glued back together. Experimental studies have shown minimal variations of the porous material properties using this technique once the adhesive material completely dried [24]. An acoustic foam block (melamine #1 if not stated otherwise) was placed on top of a shaker with the block glued to a stiff honeycomb platform (see Fig. 4). An accelerometer on top of the honeycomb platform and one on the mass inclusion allowed the transfer function between the drive acceleration at the base and the acceleration of the mass inclusion to be measured and natural frequency determined. Both accelerometers have a weight of 0.7 g. The accelerometer on top of the mass inclusion was connected using wax. It was positioned on the inclusion center and its mass was accounted for in all experiments. Fig. 4 shows the data acquisition system with the HG blanket and the shaker.

For the corroboration of the "effective area" approach (described below), three additional porous media were used: a different type of melamine foam (melamine #2), polyurethane, and polyamide. The parameters for the four types of porous material were measured and are presented in Table 1. The flow resistivity was measured using the Ingard and Dear method [25] and the elasticity taken from a dynamic shaker test [26]. The two melamine foams were acquired from two different companies and exhibit similar, although not identical, properties. The polyurethane and the polyamide parameters vary significantly from those of the melamine foam; the polyurethane has high density while the polyamide has high flow resistivity. Only "typical" values are defined since the properties of the foam can vary from sample to sample. The authors simply aim to outline a universal approach to predicting and controlling mass inclusion behavior in HG samples. It should also be noted that the foam may be anisotropic. Therefore, the method proposed here is only valid if the foam is tested with the same orientation as it is used for the manufacturer of the HG blanket.

The material properties of a nominally identical acoustic foam produced in two different batches can vary significantly and can also vary within a single batch even within the same sheet. The five porous layers with melamine #1a utilized for results in Table 2 (discussed in Section 3.2.4) were all from the same large sheet of foam. Melamine #1b comes from a different batch entirely. Experimental results provided here indicate that if the test specimens are taken across different batches of foam the standard deviation of the resulting natural frequencies is five times larger than the standard deviation if the test specimens are all selected from the same batch.

Table 2
Parameters and results from masses embedded in "melamine #1a".

Mass shape	Weight (g)	Projected area (m^2)	Effective area (m^2)	Average mean of nat. frequency (Hz)	One-sided 90% confidence interval (Hz)	Theoretical nat. frequency (Hz)
Ball	5.6	1.0×10^{-4}	0.8×10^{-3}	120.2	3.2	110.7
Coin	5.8	4.6×10^{-4}	1.6×10^{-3}	154.8	7.9	156.7
Beam	5.9	6.5×10^{-4}	2.3×10^{-3}	190.8	6.4	188.9
Square	5.9	18.0×10^{-4}	4.0×10^{-3}	240.2	8.7	246.1

3. Parametric studies

This chapter outlines vital HG blanket characteristics including the "footprint," the "mass interaction distance," and the "effective area" to allow prediction of mass inclusion behavior.

The parametric studies of the HG blanket are performed to tune the mass inclusions to the required natural frequency. There are two ways to tune a mass–spring system: changing the mass or changing the stiffness. Since the poro-elastic layer acts as a distributed spring, there are many parameters that can be varied to change the effective stiffness, and these are investigated in detail and presented in the following sections.

3.1. Tuning with varied mass

One way to tune the inclusion behavior is to change the mass of the inclusion. A foam block (melamine #1a) with dimensions 140 mm × 140 mm × 50 mm (length, width, and thickness, respectively), three inclusions, and an attached accelerometer were used. The inclusions were individually glued on top of the porous block and tested sequentially. Three different mass inclusions with the same surface shape and area were used. Mass was varied from 11.7 to 27.0 g. Fig. 5 shows the measured transfer function between the input acceleration of the base and output velocity of the three inclusions. The resonance frequency follows accepted mass law since the natural frequencies were proportional to the inverse square root of the mass (Fig. 6).

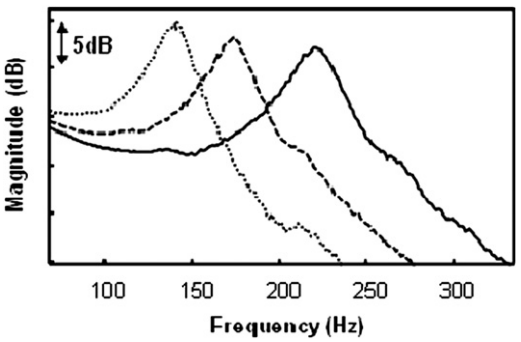

Fig. 5. Measured transfer function between the input acceleration of the base and output velocity of three different mass inclusions: 11.7 g (——), 18.7 g (– – – –), and 27 g (. . . . .).

3.2. Tuning with varied stiffness

The stiffness of the HG blanket mass–spring–damper system is created when a region of the porous media interacts with the mass inclusion. Tuning the mass inclusions by varying the stiffness is a complicated process. To accurately predict behavior, tuning with varied stiffness requires the definition of mass depth, a "footprint," "mass interaction distance," and "effective area."

3.2.1. Mass depth

Varying mass depth is the simplest way to change the stiffness and thus the natural frequency of a mass embedded in a layer of poro-elastic media like melamine #1a. Fig. 7 depicts the variation in resonant frequency of an 8 g mass in a melamine foam block (140 mm × 140 mm × 110 mm) versus layer thickness. The resonant frequency of the mass inclusion increases with decreasing depth. To indicate the trend of the natural frequency measurements, the solid line represents a curve fit through the data points given as

$$f_n = 83.42 + \frac{6.044}{\sqrt{x}} \tag{1}$$

where the resonant frequency f_n is inversely proportional to the square root of the mass depth x converging at 83.42 Hz.

Kidner et al. [27] validated this measurement in a previous experiment with a 35 mm × 35 mm × 100 mm melamine foam block. The analysis in the next section signifies that Kidner et al. used a porous block too small to take into account all stiffness effects.

3.2.2. Footprint

When varying material stiffness, the concept of the "footprint" is vital. Since the poro-elastic media acts as a distributed spring, a mass moving inside this media will have a region of influence. The poro-elastic material directly adjacent to an inclusion will move with the same displacement as the inclusion, but the motion decreases as the distance increases.

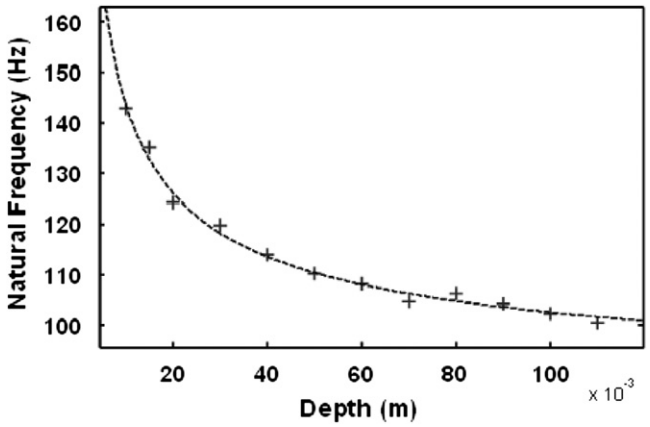

Fig. 6. Variation of resonant frequency of an 8 g mass in a melamine foam block as a function of the thickness of foam beneath the mass. Plotted are experimental measurements (+) and a curve fitted through measured data (————).

Beyond a certain distance from the inclusion the motion of the media becomes negligible. Therefore, the inclusion can be considered to have a finite region of influence, or footprint. Similarly the forces generated by the inclusion only affect a finite region on the base of the poro-elastic media. The forces are the largest directly underneath the inclusion, and increased distance from the inclusion results in decreased forces. The footprint embodies the volume of poro-elastic media that a mass inclusion influences and also delineates the stiffness. The definition of the footprint is dependent on what is considered to be a "negligible" influence, and in this manuscript a working definition of "footprint distance" is suggested. However, other definitions could also be used.

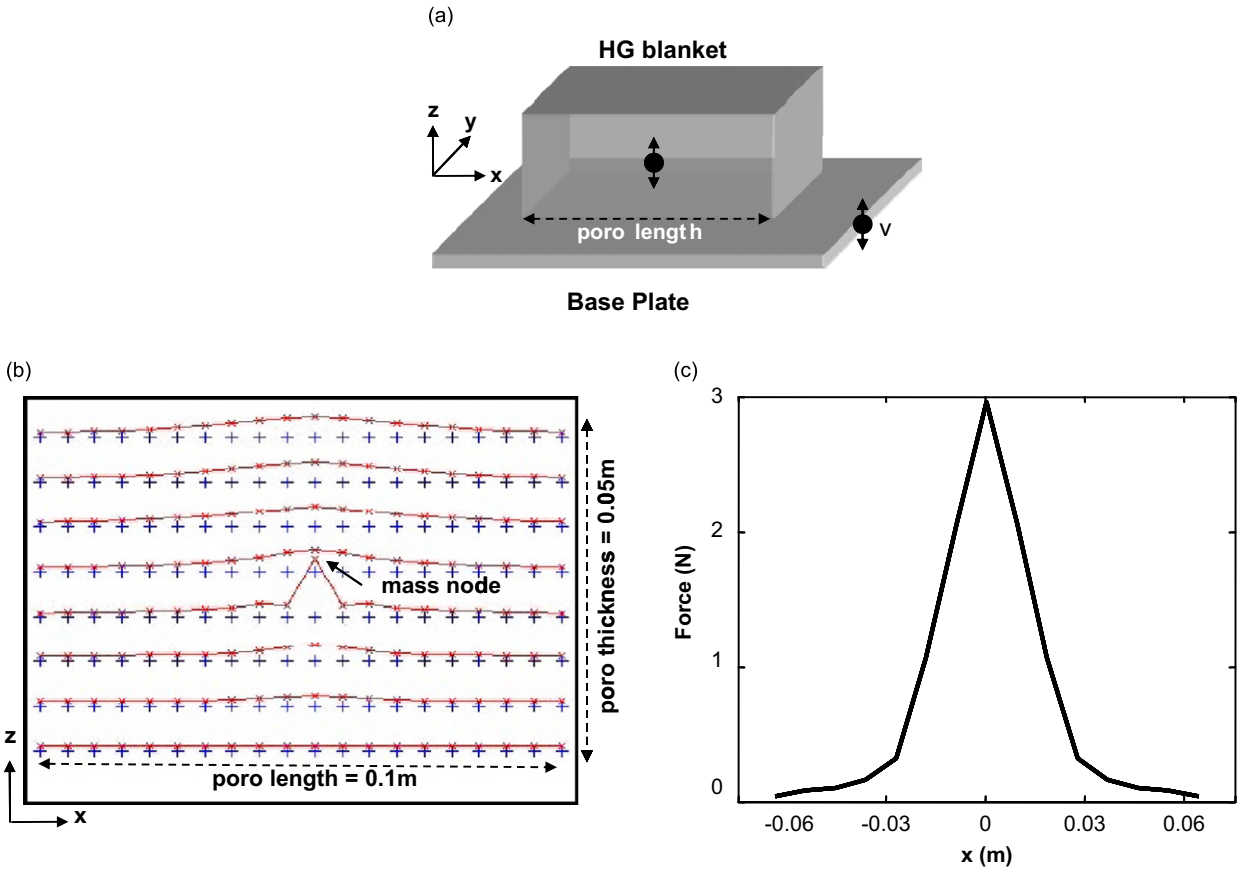

Fig. 7. (a) Schematic of the HG blanket glued on a base plate moving with the velocity v. (b) An operating deflection shape of a layer of porous media with one mass inclusion (2-D). (c) Force at the base versus the distance X from the middle of the mass inclusion placed at the center of the 150 mm × 100 mm × 50 mm poro-elastic layer, or the numerical "footprint distance" computation.

This section presents the basic concept of a footprint, defines the footprint distance, and investigates this concept in detail for a specific type of acoustic foam. However, the footprint is likely to vary for different porous materials with varied physical properties. Defining the footprint for a range of materials and for various poro-block thicknesses is a future endeavor and is beyond the scope of this document. The authors simply aim to provide a novel, systematic method to evaluate and define mass inclusion interactions and performance.

To investigate the basic behavior of a HG blanket (melamine #1a), the FE model was run with a $20 \times 8 \times 8$ uniform grid and simulated on a base plate that was driven with a uniform velocity v in the z-direction (Fig. 7(a)). Fig. 7(b) shows the operating deflection shape of the HG blanket when driven at resonance. This operating deflection shape is a cut-out of the x–z plane of the blanket at the y-coordinate corresponding to the mass position. In this example, the length and width of the block of foam are 0.1 m, and the thickness is approximately 0.05 m. The weight of the mass inclusion is 5.6 g. The nodes of the FE model in its static position are noted with +'s, and the displacements after moving the base plate are noted with $\times$'s connected with lines. A uniform velocity (and displacement) was applied to the base of the HG blanket. The lowest row of static nodes has a constant distance to the displaced node lines since they are directly attached to the base. As expected, the porous media provides less motion with greater distance from the mass. One can see that the region of influence is a non-uniform area around the mass inclusion; therefore, the footprint is a non-uniform volume considering that the operating deflection shape only shows the x–z plane of the blanket. The key is to define and compute a horizontal distance to be able to account for the interaction between the mass inclusions. This distance will be defined in the next paragraph and denoted as "footprint distance."

Similarly, Fig. 7(c) shows a plot of the force at the base versus the horizontal distance X from the mass inclusion that is placed at the center of a 140 mm $\times$ 140 mm $\times$ 90 mm (length, width, and thickness, respectively) poro-elastic layer. The plot shows that the maximum force is directly below the mass and drops down to 5% of the maximum force at a distance of approximately X=0.04 m. Therefore this distance can be used as a working definition of the footprint distance.

In order to determine the footprint distance experimentally and to verify mathematical results presented, a shaker experiment was chosen with the allocations shown in Fig. 4. A mass inclusion inside a very small porous block with length and width much smaller than the footprint should experience lower stiffness than an inclusion embedded inside a porous layer with infinite x and y dimensions. Increasing the x and y dimensions of a small block of porous material with an inclusion should lead to an increase in the natural frequency (i.e. more stiffness). This increase will continue until the

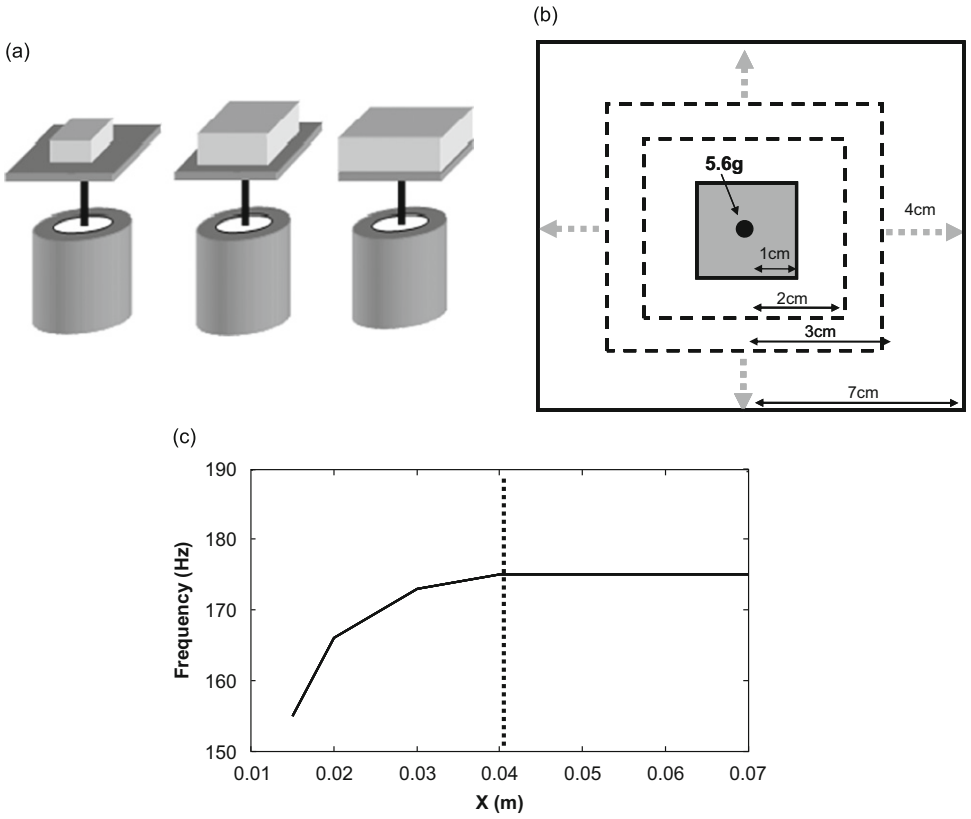

Fig. 8. (a) Schematic of the experimental "footprint distance" measurement, (b) dimensions of the poro-elastic layer, and (c) natural frequency versus the distance X of the experimental "footprint distance" measurement.

dimensions of the poro-block reach the volume in which the inclusions interact, i.e. the footprint. Above this dimension, the natural frequency of the mass inclusion should not change significantly. Fig. 8(a) shows a schematic of this concept. A block of melamine foam with a 5.6 g mass embedded in the center position was used in the experimental design shown in Fig. 4. Fig. 8(b) shows the top view of the porous block. As with the mathematical example, the dimensions are 140 mm × 140 mm × 91 mm (length, width, and thickness, respectively). The measurement was repeated while holding the thickness constant and cutting 10 mm off on each of the sides. For the last measurement, only 5 mm was removed. Consequently, the maximum distance X from the center of the mass inclusion to the side of the poro-block is 7 cm. The distance X for the second measurement was 6 cm, and the remainder followed the same trend. Fig. 8(c) shows the experimentally determined natural frequency versus the distance X. At X=0.07 m, the natural frequency is higher than the one at X=0.015 m due to previously described stiffness effects. At X=0.04 m the natural frequency of the embedded mass converges to 175 Hz, indicating that the natural frequency does not increase significantly with enlargement of foam block dimensions beyond this point. Thus, the footprint distance can be considered to be approximately 0.04 m for this case and is in agreement with the numerically computed footprint distance described above. The results presented in Fig. 8(c) also indicate that boundary conditions have a significant effect on the natural frequency unless the mass is farther away from the boundary than the footprint.

3.2.3. *Mass interaction distance*

When designing the HG blanket, inclusion interactions within a block of poro-elastic material (like melamine #1a) are important. Two inclusions positioned a large distance from each other within a porous layer will not interact, but two inclusions directly next to each other will interact a great deal or even act as one large mass, contributing a large impact on the natural frequency of the HG blanket. The FE model of the porous material presented in Section 2.1 is used to investigate the distance when the two mass inclusions are independent of each other, the "mass interaction distance." A foam block of dimensions 200 mm × 100 mm × 100 mm (length, width, and thickness, respectively) with a 21 × 7 × 7 FE grid was used with two 5.6 g mass inclusions. The previous section showed that the footprint distance for a 5.6 g inclusion in melamine foam is approximately 0.04 m. One mass inclusion was positioned 0.04 m from the side of the foam in a center-depth position, and the second mass inclusion was positioned 0.12 m away. In this configuration there are two identical natural frequencies, one for each of the masses. However, as the second mass is moved closer to the first, the masses become coupled and the system must now be considered to have *two modes* of vibration, each with a different natural frequency (see Fig. 9(a)). The natural frequencies for the two modes were computed for various separation distances and are presented in Fig. 9(b). One would expect that the inclusions stop interacting when the two footprints no longer overlap, and the two modal natural frequencies should converge to the uncoupled natural frequencies. When the inclusions are very close together, the natural frequency of one mode (masses moving out of phase) will tend to infinity, but the second mode (masses moving in phase) will tend towards the natural frequency of a single inclusion with twice the mass. This is demonstrated in Fig. 9(b), and the masses stop interacting when they are 0.085 m away from each other, where the mass interaction distance is roughly twice the footprint distance.

3.2.4. *Effective area*

Masses embedded inside a porous layer interact with a certain volume of the porous media. However, the footprint may change if the mass shape is changed. By increasing the surface area of an inclusion (i.e. its projected area), it can be

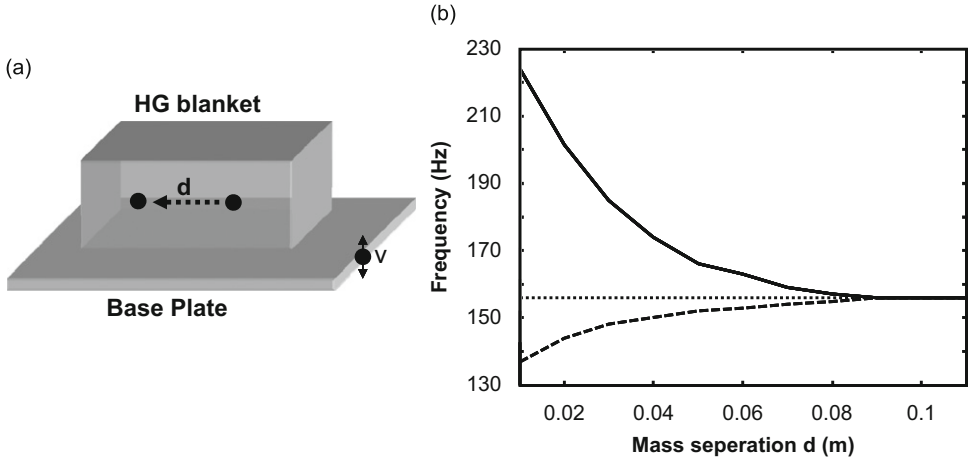

Fig. 9. (a) Schematic of numerical estimation of "mass interaction distance" and (b) FE results of natural frequencies of mass inclusions versus mass separation. Plotted is the mode of the first mass (——), the mode of the second mass (– – – –), and the natural frequency of a single mass by itself (……).

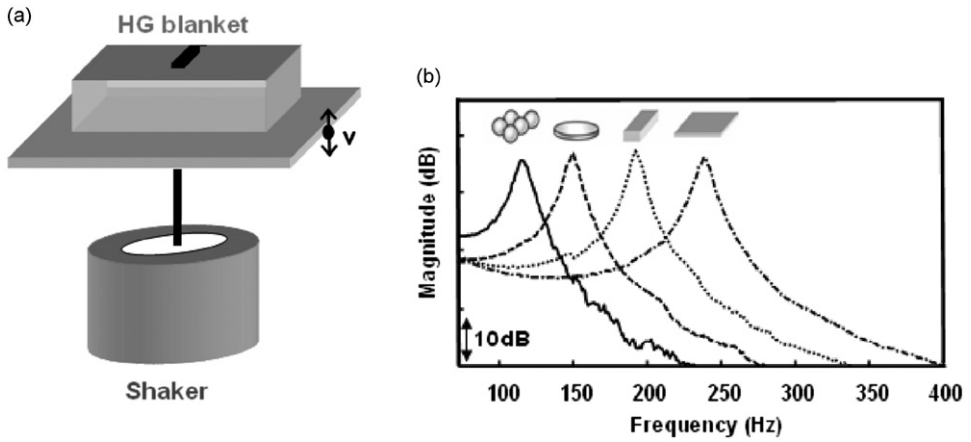

Fig. 10. (a) Schematic of the HG blanket experiments used for the "effective area" experiments and (b) natural frequencies of different mass shapes measured in shaker experiment. 5.6 g ball (——), 5.8 g coin (— — —), 5.8 g beam (……), and 5.9 g square (-·-·-·-·-·-·-).

expected to interact with a larger volume of the porous media. Therefore, the stiffness of the mass–spring–damper system inside the HG blanket is expected to increase. A shaker experiment, similar to the one shown in Fig. 4, was used to measure the natural frequencies of four inclusions with different shapes yet with similar mass. Fig. 10(a) shows a scheme of the HG blanket used in the shaker experiment with a mass glued on the top of the porous block.

Table 2 displays the result of this experiment. The first two columns show the mass and the projected area of the mass shapes. The ball, the beam, and the square have significantly different projected areas. The projected area of the beam and the coin, however, are roughly the same.

Fig. 10(b) presents the transfer functions between the input acceleration of the base and output velocity of the four mass inclusions. Each measurement was repeated five times using five different blocks of melamine foam #1a. The mean and the one-sided confidence interval with a 90% probability are shown in Table 2. The maximum deviation of the natural frequency is below 9 Hz for all of the mass shapes (with a probability of 90%). As expected, the natural frequency increases when the area of the masses is increased. Although the areas of the beam and the coin are very similar, the natural frequency of the coin is interestingly significantly lower than the natural frequency of the beam. The results presented in Fig. 10(b) and Table 2 indicate that the natural frequency does not simply change linearly with projected area but also is dependent on the *shape* of the inclusion.

As a first-order approximation, the stiffness of the mass inclusion can be considered to change with an "effective area" that is defined in Fig. 11(a) as a distance d away from the perimeter of the projected area. Consequently, the "effective area" of a beam with the same projected area as a coin would result in a significantly larger "effective area" and consequently in a larger footprint and stiffness. This approximation assumes that the equivalent stiffness constant k_{eq} in the mass–spring–damper system inside the HG blanket is a function of the effective area $a(d)$ and a porous material constant c_{poro}:

$$k_{eq} = a(d)c_{poro} \tag{2}$$

Given the porous material constant c_{poro}, the distance d and the mass weight m, one can compute the natural frequency in Hz

$$f_n = \frac{1}{2\pi}\sqrt{\frac{a(d)c_{poro}}{m}} \tag{3}$$

Fig. 11(b) shows the projected areas as a function of measured natural frequencies (× 's connected with the solid line). The dashed line is the approximation of the natural frequencies plotted as a function of effective area using Eq. (3). A family of curves with different d's and c_{poro}'s was plotted, and the dashed curve in Fig. 11(b) is the curve with the best fit through all measurements. The distance d that best fits the data is used to calculate the effective areas listed in Table 2 and is 0.0105 m with $c_{poro}=3.9\times10^6\,N/m^3$.

To define this method as a universal predictive tool, a second type of melamine foam block, melamine #1b, with different material properties was studied. The porous block used in the previous experiments is denoted melamine #1a.

In order to predict the natural frequency as described in Eq. (3), one must define the distance d and the material property c_{poro}. The c_{poro} depends on the material properties of the porous material used, but the distance d depends on geometry and is not strongly affected by small changes in the material properties. Therefore, d is assumed to be equal for melamine #1a and melamine #1b. Measurement of only c_{poro} is needed to predict the natural frequency for a given mass shape (i.e. effective area). In order to determine c_{poro} for melamine #1b, the natural frequencies of the beam and the coin

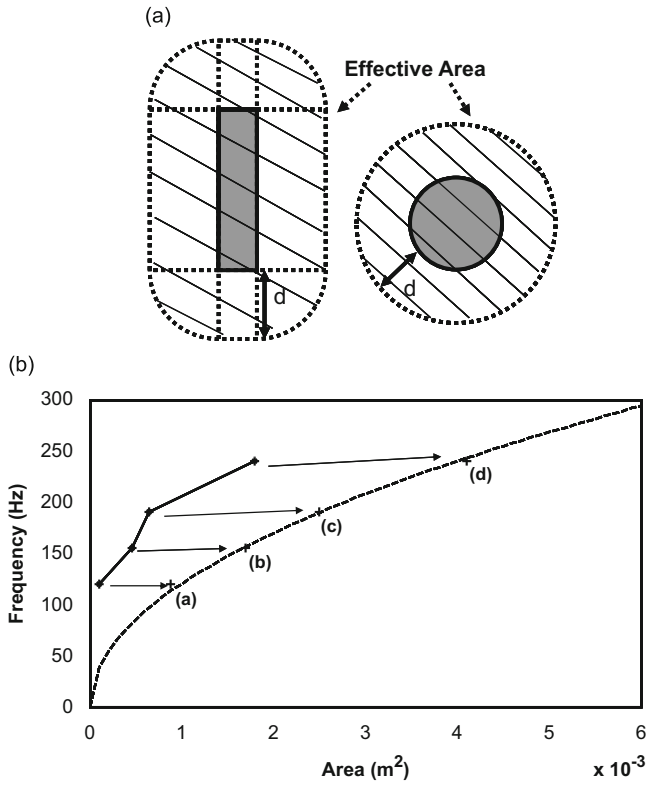

Fig. 11. (a) Schematic of the "effective area" concept and (b) comparison of the "projected" (▬▬) and the predicted "effective area" (– – – –) along with the measurements (+) of the ball (a), coin (b), beam (c), and square (d) versus frequency.

were measured using the same experimental design used in the previous test on poro #1. Eq. (3) was then used to calculate c_{poro} as $8.2 \times 10^6\,N/m^3$. Note that only one measurement, either of the coin or the beam, is needed to compute c_{poro}. However, a best fit between the two points was used.

Fig. 12 shows a plot with the two theoretical curves of the natural frequencies as a function of effective areas of the mass inclusions of melamine #1a (dashed) and melamine #1b (dotted). The already presented natural frequencies of melamine #1a are noted as $\times$'s, identically to Fig. 11(b). The measured natural frequencies of the beam and the coin glued to melamine #1b are noted with squares. As the second step, the natural frequencies of the ball and the plate glued to melamine #1b were measured. Both lie on top of the predicted dotted curve in Fig. 12, noted as circles. The proposed

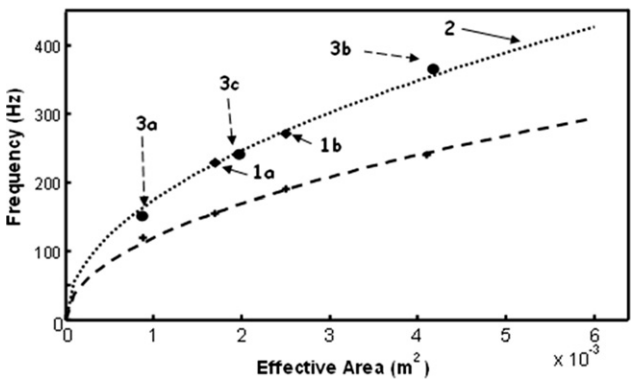

Fig. 12. Experimental validation of "effective area" approach. Shown is the predicted natural frequency for melamine #1a (– – – –) along with the measurements (+). The coin (1a) and beam (1b) measurement for melamine #1b were used to plot prediction (2, ……) for the ball (3a), square (3b) and an additional shape, a triangle (3c).

Table 3
Parameters and results from masses embedded in "melamine #1b".

Mass shape	Weight (g)	Projected area (m^2)	Effective area (m^2)	Nat. frequency (Hz)	Theoretical nat. frequency (Hz)
Ball	5.6	1.0×10^{-4}	0.8×10^{-3}	150	161.1
Coin	5.8	4.6×10^{-4}	1.6×10^{-3}	230	227.5
Beam	5.9	6.5×10^{-4}	2.3×10^{-3}	270	274.9
Square	5.9	18.0×10^{-4}	4.0×10^{-3}	370	358.1
Triangle	6.1	4.9×10^{-4}	2.0×10^{-3}	249	252.5

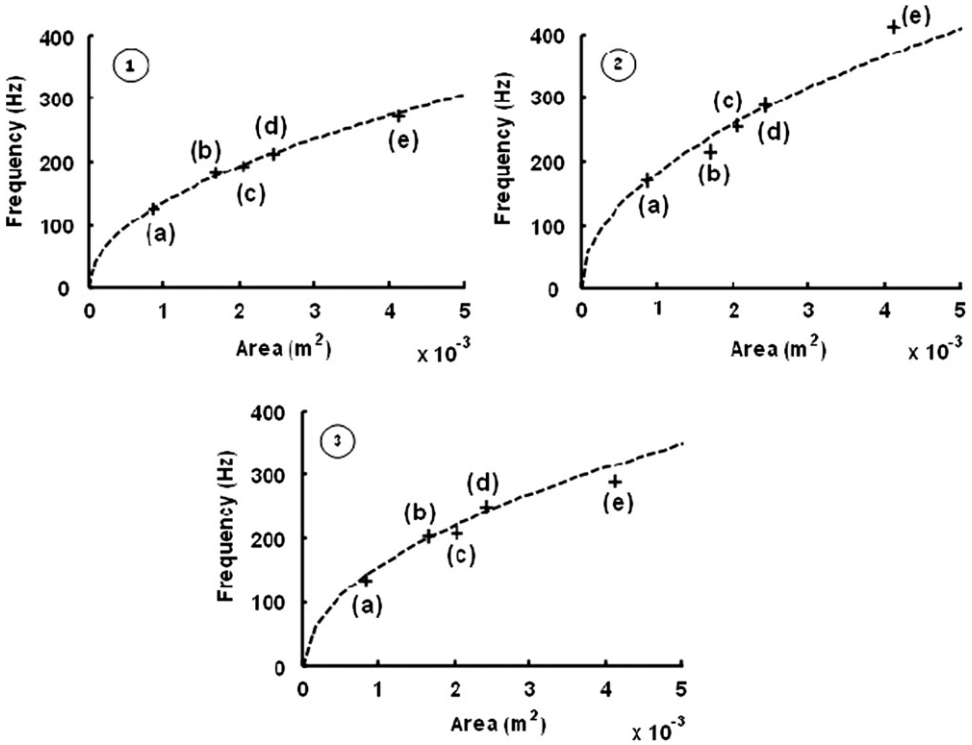

Fig. 13. Comparison of theory (————) and experiment (+) of "effective area" approach with (1) melamine foam, (2) polyamide, and (3) polyurethane. Measured are the natural frequencies of ball (a), coin (b), triangle (c), beam (d), and square (e).

formula works for porous media with the four mass shapes: ball, coin, beam, and plate. In addition, a "new" mass shape, a triangle with roughly the same weight as the other masses, is introduced. The "effective area" of the triangle lies between the "effective area" of the coin and the beam. The natural frequency was measured and plotted in Fig. 12 and is shown to lie within 2% of the predicted value, further validating this approach. The results are summarized in Table 3.

To prove that the "effective area" approach is not only valid for one type of porous medium, three additional types of acoustic foam were used: melamine foam #2, polyamide, and polyurethane. These three types of porous media are some of the most common materials used for interior-noise-control applications. Fig. 13 (1) shows the comparison of the predicted and the experimental natural frequency of five mass inclusions (a: ball, b: coin, c: triangle, d: beam, e: square plate) versus the effective area for the melamine foam #2. All five mass shapes have the same weight of approximately 6 g. The natural frequencies of the mass inclusions inside the melamine foam remain close to the predicted curve with a maximum error of 5 Hz. Furthermore, Fig. 13 presents the validation for polyamide (2) and polyurethane (3). Both plots show excellent correlation between theory and experiment. The experiments for polyamide were executed carefully due to the compressibility of this porous media. However, polyurethane use was in accordance with the use of melamine foam.

In conclusion, the "effective area" approach was validated for three of the most commonly used porous media: polyamide, polyurethane, and melamine foam. The results presented indicate a major step towards making the HG

blankets a serviceable treatment for interior-noise-control applications. Using this approach, the natural frequencies of the mass inclusions inside the HG blanket can be controlled entirely by changing the shape of the inclusion. This approach allows all of the inclusions to be placed on one layer instead of varying the depth, and this method will make the blankets much easier to manufacture. In addition, the use of the "effective area" theory is not limited to a certain type of melamine but is applicable to a variety of foams. Most importantly the proposed effective area approach, used to explain the natural frequency of different mass shapes with constant embedded mass in porous media, has a maximum error of 8% for all the predictions made in this manuscript.

4. Conclusions

This manuscript presented a mathematical and experimental study of the behavior of mass inclusions placed inside a poro-elastic media. The inclusions were shown to interact with a finite volume of the poro-elastic media, termed the "footprint," and it was shown that this footprint impacted the tuning frequency of the mass inclusion and the interaction distance between multiple masses. Inclusion mass and depth were shown to alter the natural frequency of the inclusion. Both the area and shape of the inclusion controlled the natural frequency through changing the footprint.

A novel, empirical "effective area" approach to predict the natural frequency of different mass shapes embedded in porous media was found and experimentally verified for many different types of porous media, including melamine foam, polyurethane, and polyamide. A maximum error of 8% existed for all the predictions made in this document.

By defining effective mass inclusion parameters, novel property control methodologies for HG blanket materials were discovered that allow better control of natural frequencies through controlling the mass, depth, area, and shape of the inclusions. In principle, inclusions of various shapes placed on a single layer in the foam can be used to control a wide range of frequencies, and this concept will make the blankets much easier to manufacture.

Acknowledgments

This project was supported by SMD Corporation under a NASA SBIR Grant A2.04-9836. In particular the support and collaboration of Prof. Rob Clark, Dr. Curtis Mitchell, Prof. Chris Fuller, Dr. Mike Kidner, Dr. Haisam Osman, Dr. Alessandro Toso, Florian Boess, Holger Werschnik, Thomas Funke, Andreas Wagner, and David Bartylla are gratefully acknowledged.

References

[1] J.F. Wilby, Aircraft interior noise, *Journal of Sound and Vibration* 190 (1996) 545–564.
[2] H. Baumgartl, Lightweight, versatile all-rounder, *Kunststoffe International* 96 (2006) 78–82.
[3] K.E. Heitman, J.S. Mixson, Laboratory study of cabin acoustic treatments installed in an aircraft fuselage, *Journal of Aircraft* 23 (1986) 32–38.
[4] J.S. Mixson, L.A. Roussos, C.K. Barton, R. Vaicaitis, M. Slazak, Laboratory study of add-on treatments for interior noise control in light aircraft, *Journal of Aircraft* 20 (1983) 516–522.
[5] J.P. Carneal, Active Structural Acoustic Control of Double-panel Systems including Hierarchical Control Approaches, PhD Thesis, Virginia Polytechnic Institute and State University, 1996.
[6] P. Gardonio, S.J. Elliott, Active control of structure-borne and airborne sound transmission through double-panel, *Journal of Aircraft* 36 (1999) 1023–1032.
[7] P.A. Nelson, S.J. Elliott, *Active Control of Sound*, Academic Press, London, 1993.
[8] M. Brennan, Vibration control using a tunable vibration neutralizer, *Journal of Mechanical Engineering Science, Proceedings of the Institution of Mechanical Engineers* 211 (Part C) (1997) 91–108.
[9] S.M. Lee, Normal vibration frequencies of a rectangular two-dimensional array of identical point masses, *Journal of Sound and Vibration* (1976) 595–600.
[10] D.M. Photiadis, Acoustics of a fluid loaded plate with attached oscillators, part 1: Feynman rules, *Journal of the Acoustical Society of America* 102 (1997) 348–357.
[11] C.R. Fuller, M.R.F. Kidner, X. Li, C.H. Hansen, Active–passive heterogeneous blankets for control of vibration and sound radiation, *Proceedings of the Active 04*, Williamsburg, VA, September 20–24, 2004.
[12] M.R.F. Kidner, C.R. Fuller, B. Gardner, Increase in transmission loss of single panels by addition of mass inclusions to a poro-elastic layer: experimental investigation, *Journal of Sound and Vibration* 294 (2006) 466–472.
[13] F. Sgard, N. Atalla, C.K. Amedin, Vibro-acoustic behavior of a cavity backed by a plate coated with a meso-heterogeneous porous material, *Acta Acustica United with Acustica* 93 (2007) 106–114.
[14] N. Atalla, C.K. Amedin, F. Sgard, Numerical and experimental investigation of the vibro-acoustics of a plate backed cavity coated with a heterogeneous porous material, SAE Meeting, Traverse City, USA, 2003, 2003-01-1453.
[15] W.T. Thomson, *Vibration Theory and Applications*, Prentice-Hall Inc., Englewood Cliffs, NJ, 1965.
[16] J. Ormondroyd, J.P. Den Hartog, Theory of the dynamic vibration absorber, *Transactions of the ASME* 50 (1928) 9–22.
[17] J.P. Den Hartog, *Mechanical Vibrations*, Dover Publications, McGraw-Hill, New York, NY, 1934.
[18] R. Panneton, N. Atalla, An efficient finite element scheme for solving the three-dimensional poro-elastic problem in acoustics, *Journal of the Acoustical Society of America* 101 (1997) 3287–3298.
[19] M.A. Biot, Theory of propagation of elastic waves in a fluid-saturated porous solid. I. Low-frequency range, *Journal of the Acoustical Society of America* 28 (1956) 168–178.
[20] J.F. Allard, *Propagation of Sound in Porous Media: Modelling Sound Absorbing Materials*, Elsevier Science Publishers Ltd., London and New York, 1993.
[21] A. Gautam, Design and Development of Advanced Vibration and Noise Control Devices Using Finite Element Analysis, Thesis, Virginia Polytechnic Institute and State University, 2005.
[22] K. Idrisi, M.E. Johnson, J.P. Carneal, Passive control of sound transmission through a double panel using heterogeneous (HG) blankets, part I: Modeling and validation, *Proceedings of the Noise-Con 2007*, Reno Nevada, October 22–24, 2007.

[23] K. Idrisi, M.E. Johnson, J.P. Carneal, Control of aircraft interior noise using heterogeneous (HG) blankets, *Proceedings of the Meetings on Acoustics* 1 (2008) 065001.
[24] K. Idrisi, Heterogeneous (HG) Blankets for Improved Aircraft Interior Noise Reduction, PhD Thesis, Virginia Polytechnic Institute and State University, 2008.
[25] K.U. Ingard, T.A. Dear, Measurements of acoustic flow resistance, *Journal of Sound and Vibration* 103 (1985) 567–572.
[26] J. Park, Measurements of the frame acoustic properties of porous and granular materials, *Journal of the Acoustical Society of America* 118 (2005) 3483–3490.
[27] M.R.F. Kidner, K. Idrisi, M.E. Johnson, J.P. Carneal, Comparison of experimental, finite element and wave based models for mass inclusions in poro-elastic layers, *Proceedings of the ICSV 14*, Cairns, Australia, 2007, Paper 577: www1-www8.